TÜBİTAK

Turkish J. Eng. Env. Sci.
36 (2012) , 45 – 58.

doi:10.3906/muh-1007-140

Effect of porous screen on flow stabilization and heat transfer in a channel using variable porosity model by the lattice Boltzmann method

Arman HASANPOUR[1], **Koroush SEDIGHI**[2], **Mousa FARHADI**[2,*]
[1] *Young Researchers Club, Gorgan Branch, Islamic Azad University, Gorgan-IRAN*
[2] *Faculty of Mechanical Engineering, Babol Noshirvani University of Technology, Babol-IRAN*
e-mail: mfarhadi@nit.ac.ir

Received: 27.07.2010

Abstract

Boltzmann method. The flow in the porous screen was simulated by the Brinkman-Forchheimer model. Numerical solutions were obtained for variable porosity models, and the effect of the Darcy number and porosity were studied in detail. Results showed that the stabilization of the flow field and heat transfer were dependent on the Darcy number. Distribution of the stream field became more stable when the Darcy number decreased. Moreover, the temperature distribution was more homogeneous at lower Darcy numbers and porosity values. Results showed that the effect of variable porosity was significant in the neighborhood of the solid boundary. In addition, dissimilarity between constant and variable porosity models was decreased by Darcy number reduction.

Key Words: Lattice boltzmann method, porous media, variable porosity model, nonuniform flow

1. Introduction

Channels filled with porous matrices have been widely used in a variety of engineering applications, including flow stabilizers in burners, torches, and advanced air conditioning systems. Many researchers have investigated fluid flow and convective heat transfer in channels fully and partially filled with a porous medium (Poulikakos and Kazmierczak, 1987; Guo et al., 1997; Özdemir and Özgüç, 1997; Hamdan et al., 2000; Alkam et al., 2002; Jiang et al., 2004; Jen and Yan, 2005; Liou, 2005; Satyamurty and Bhargavi, 2010).

Poulikakos and Kazmierczak (1987) theoretically considered fully developed convection between 2 parallel plates and in a circular tube partly filled with a porous matrix adhered to the wall. Porosity variation of a porous medium consisting of screen mesh layers was determined experimentally by Özdemir and Özgüç (1997). The volume element that gives the same result approximately at each point of the medium, except the wall region, is considered to be the representative elementary volume (REV) of that medium. Guo et al. (1997) numerically studied pulsating flow in a pipe partially filled with a porous medium by the finite volume method. In their

*Corresponding author

work, they fitted the porous to the pipe wall. Hamdan et al. (2000) studied forced convection by inserting a porous substrate into the core of a parallel-plate channel numerically. Alkam et al. (2002) considered forced convection flow in a channel partially filled with porous layers on the top and bottom walls. Their results showed that the existence of the porous substrate improved the Nusselt number. The effects of variable porosity and the physical properties of fluid on forced convective heat transfer in sintered porous plate channels were simulated numerically by Jiang et al. (2004). Jen and Yan (2005) used a vorticity-velocity method to simulate the fluid flow and heat transfer in a channel partially filled with a porous medium. In their investigation, the friction factor and Nusselt number were presented as a function of axial position. Liou (2005) proposed a new numerical technique for simulating flow in porous media in terms of pore-scale analysis. The effect of a wall-mounted porous layer in the channel over the heat transfer was investigated by Satyamurty and Bhargavi (2010). The variable porosity model has been used for engineering and technical applications. Chandrasekhars and Radha (1988) studied the effect of variable porosity on laminar forced convection in a regularly heated vertical porous channel using an exponential function. They observed that the heat transfer rate was increased by increasing the porous parameter. The effect of the porosity variation of the gas diffuser layer on the performance of a proton exchange membrane fuel cell was reported by Chu et al. (2003). This analysis is necessary due to the presence of liquid water in the gas diffuser layer, which causes the nonuniform porosity distribution. Alazmi and Vafai (2004) investigated the effect of variable porosity and thermal dispersion on free surface flow through porous media. They concluded that the effect of variable porosity is not considerable, except near the walls.

The lattice Boltzmann method (LBM) is a useful technique for simulating fluid flow and heat transfer (Succi et al., 1989; Seta and Kono, 2004; Hamdan et al., 2000; Delavar et al., 2009, 2010). This method has been successfully applied to flow modeling in porous media. The most common approach to applying the LBM to porous flow is to model the flow in the REV scale (Nield and Bejan, 2006). This is accomplished by including an additional term in the standard lattice Boltzmann equation. Spaid and Phelan (1997) proposed a model based on the Brinkman equation for single-component flow in porous media. Although the Brinkman model has been used to describe flow in porous media, some limitations still exist in this model (Kim and Vafai, 1989).

In this study, linear and nonlinear matrix drag components were considered as well as the inertial and viscous forces using the Brinkman-Forchheimer model (Guo et al., 2002; Nield and Bejan, 2006). The main objective of the present work was to investigate the effect of a porous screen on the stability of flow field and heat transfer with nonuniform inlet velocity and temperature in a channel using the LBM. The mathematical formulations for porous media were based on the Brinkman-Forchheimer model (Guo and Zhao, 2002). Results were obtained for constant and variable porosity models, and the effects of the Darcy number and porosity were considered.

2. Mathematical model

Flow and heat transfer in a horizontal plane channel with a porous screen were simulated by the LBM. The channel height and length were H and L = 8H, respectively, and nonuniform velocity and temperature were considered at the inlet (Figure 1). At the inlet, the velocity ratio was $\frac{U_1}{U_2} = 15$; the dimensionless inlet temperature was $\theta_1 = 1$, $\theta_2 = 0$; and the wall dimensionless temperature was $\theta_w = 0$. The porous sample was assumed to be saturated with a fluid that was in local thermal equilibrium (LTE) with the solid matrix (Kaviany, 1985). The porous screen was located at a distance of 0.5H from the entrance of the channel with a width equal to 0.2H.

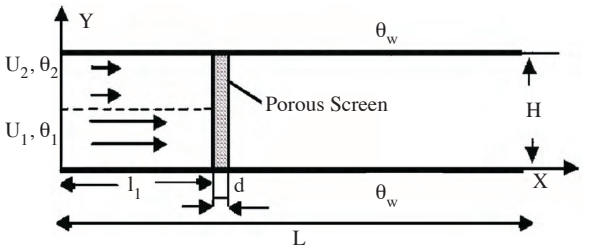

Figure 1. Geometry of the problem.

3. Lattice Boltzmann method in porous media

The LBM for incompressible fluid flow in porous media has been proposed by several researchers (Guo and Zhao, 2002; Mohammad, 2002; Seta et al., 2006).

In the LBM, the fluid is modeled by a single-particle distribution function. The distribution functions for porous media are governed by the lattice Boltzmann equation, as follows (Guo and Zhao, 2002):

$$f_i\left(\vec{x}+\vec{e}_i\delta_t, t+\delta_t\right) = f_i\left(\vec{x},t\right) - \frac{f_i\left(\vec{x},t\right) - f_i^{eq}\left(\vec{x},t\right)}{\tau_v} + \delta_t F_i. \tag{1}$$

$$g_i\left(\vec{x}+\vec{e}_i\delta_t, t+\delta_t\right) = g_i\left(\vec{x},t\right) - \frac{g_i\left(\vec{x},t\right) - g_i^{eq}\left(\vec{x},t\right)}{\tau_c} \tag{2}$$

For the $\mathrm{D_2Q_9}$ model, the discrete velocities are defined below.

$$\vec{e}_i = \begin{cases} (0,0) & \text{for} \quad i=0 \\ \left(\cos[(i-1)\frac{\pi}{4}, \sin[(i-1)\frac{\pi}{4}\right) & \text{for} \quad i=0...4 \\ \sqrt{2}\left(\cos[(i-1)\frac{\pi}{4}, \sin[(i-1)\frac{\pi}{4}\right) & \text{for} \quad i=5...8 \end{cases} \tag{3}$$

Here, δ_t is the lattice time step. The equilibrium functions for the density distribution function (f_i^{eq}) for the $\mathrm{D_2Q_9}$ model in the presence of porous media is:

$$f_i^{eq} = \left\{ \omega_i \rho \left[1 + \frac{\vec{e}_i.\vec{u}}{c_S^2} + \frac{(\vec{e}_i.\vec{u})^2}{2\varepsilon\, c_S^4} - \frac{|\vec{u}|^2}{2\varepsilon\, c_S^2} \right] \right\}, \tag{4}$$

where ε is the porosity of the porous medium and ω_i is the weighting factor. c_s is the speed of the sound and is defined by $c_s = \frac{c}{\sqrt{3}}$. The weighting factors are:

$$\omega_i = \left\{ \frac{4}{9}\ for\ i=0,\ \frac{1}{9}\ for\ i=1...4,\ \frac{1}{36}\ for\ i=5...8 \right\} \tag{5}$$

Similarly, the equilibrium distribution functions for the thermal energy distribution presented by Mohammad, g_i^{eq}, can be written as follows (Mohammad, 2007):

$$g_i^{eq} = \omega_i T \left(1 + \frac{1}{c_s^2} \vec{e}_i.\vec{u} \right). \tag{6}$$

The Brinkman-Forchheimer equation is (Seta et al., 2006):

$$\frac{\partial \vec{u}}{\partial t} + (\vec{u}.\nabla)(\frac{\vec{u}}{\varepsilon}) = -\frac{1}{\rho_f}\nabla(\varepsilon P) + \upsilon\nabla^2 u + \vec{F}. \tag{7}$$

Here, $p = \frac{\rho c^2}{3\varepsilon}$ and viscosity $\upsilon = c^2(\tau_\upsilon - 0.5)\frac{\delta_t}{3}$. The body force is expressed below (Ergun, 1952; Guo et al., 2002a).

$$\vec{F} = -\frac{\varepsilon\upsilon}{K}\vec{u} - \frac{\varepsilon.F_\varepsilon}{\sqrt{\mathrm{K}}}|u|\,\vec{u} + \varepsilon\vec{G} \tag{8}$$

$$K = DaH^2, \qquad F_\varepsilon = \frac{1.75}{\sqrt{150\varepsilon^3}} \tag{9}$$

Here, $K$is the permeability, $G$is the acceleration due to gravity, Da is the Darcy number, and $H$is the characteristic length. The total body force ($\vec{F}$) encompasses the viscous diffusion, the inertia due to the presence of a porous medium, and the external force. The suitable choice for the forcing term, F_i from Eq. (1), to obtain the correct equations of hydrodynamics is as follows (Guo and Zhao, 2002; Seta et al., 2006):

$$F_i = \omega_i\rho(1 - \frac{1}{2\tau_\upsilon})\left[\frac{\vec{e}_i.\vec{F}}{c_s^2} + \frac{(\vec{u}.\vec{F} : \vec{e}_i\vec{e}_i)}{\varepsilon c_s^4} - \frac{\vec{u}.\vec{F}}{\varepsilon c_s^2}\right]. \tag{10}$$

The fluid velocity $\vec{u}$ is defined as follows (Guo and Zhao, 2002):

$$\rho\vec{u} = \sum\nolimits_i \vec{e}_i f_i + \frac{\delta_t}{2}\rho\,\vec{F}. \tag{11}$$

As shown in Eq. (8), $\vec{F}$contains velocity $\vec{u}$. Eq. (11) is a nonlinear equation with respect to velocity $\vec{u}$. This nonlinearity is ignored by the definition of temporal velocity $\vec{v}$ (Guo and Zhao, 2002), shown below.

$$\vec{u} = \frac{\vec{v}}{c_0 + \sqrt{c_0^2 + c_1|\vec{v}|}} \qquad \vec{v} = \frac{\sum_i \vec{e}_i f_i}{\rho} + \frac{\delta_t}{2}\varepsilon\,\vec{G} \tag{12}$$

$$c_0 = \frac{1}{2}(1 + \frac{\delta_t}{2}\varepsilon\frac{\upsilon}{K}) \qquad c_1 = \frac{\delta_t}{2}\varepsilon\frac{1.75}{\sqrt{150\varepsilon^3 K}} \tag{13}$$

The fluid density and temperature are defined as:

$$\rho = \sum_i f_i, T = \sum_i g_i. \tag{14}$$

Through the Chapman-Enskog procedure, in the limit of small Mach numbers, Eq. (1) recovers the continuity equation (Seta and Kono, 2002):

$$\nabla.u = 0. \tag{15}$$

Eq. (2) describes the evolution of the thermal energy and leads to the following energy equation:

$$\frac{\partial T}{\partial t} + \nabla.(\vec{u}T) = \alpha\nabla^2 T \tag{16}$$

whereα is the thermal diffusivity, which is defined as $\alpha = c_s^2(\tau_c - \frac{1}{2})$.

Zou and He's velocity boundary condition (Zou and He, 1997) and the extrapolation boundary scheme (Guo et al., 2002b) are applied at the inlet and outlet, respectively. The second-order bounce-back boundary rule for the nonequilibrium distribution function (Zou and He, 1997) is employed for the top and bottom walls.

4. Numerical procedure

4.1. Convergence criterion

The velocity and temperature of the last step is calculated and the convergence criterion is applied to them for assurance that the convergence happens. If these parameters satisfy this criterion, the program code will go to the next step and the iterations will continue. Generally, the proper equations define the investigation of the convergence situation for the numerical methods. In other words, the error functions are used for assurance that a parameter like velocity or temperature converges. In this paper, an error function based on macroscopic parameters is applied (Figure 2).

$$\text{Error} = \frac{\sum_{i,j} \sqrt{(u_i^n - u_i^{n-1})^2 + (u_j^n - u_j^{n-1})^2}}{\sum\limits_{i,j} \sqrt{(u_i^{n-1})^2 - (u_j^{n-1})^2}} \leq 10^{-6} \tag{17}$$

If the above relationship is satisfied, the procedure of the numerical solution will continue to the next time step.

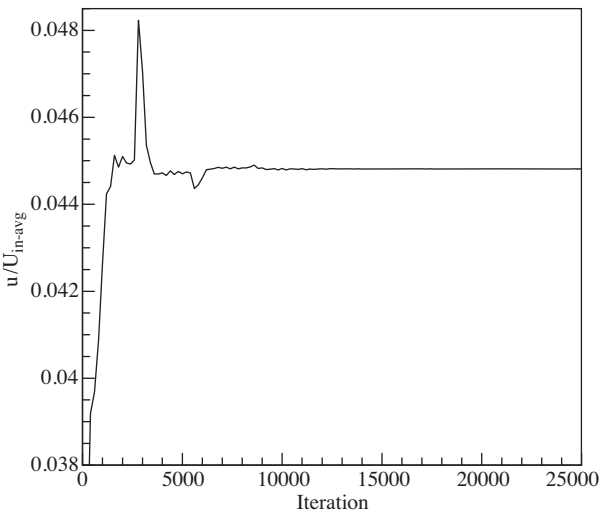

Figure 2. Velocity at x,y = H/2 at the porous screen outlet versus the iteration number.

The velocity magnitude on the positions of x = H/2 and y = H/2 of the porous screen outlet is depicted in respect to the iteration of time steps in Figure 2, which shows that after 25,000 iterations, the fluctuations disappeared and a steady state situation occurred. This means that the error function was satisfied in this iteration. The convergence of the numerical solution of the temperature profile follows the same procedure.

4.2. Boundary conditions

The schematic scheme of the mentioned problem is shown for the n × m computational domain. The solid walls are assumed to be noslip; thus the bounce-back scheme is applied to them excluding the top wall. Zou and He's known velocity condition and the extrapolation boundary condition are used for the inlet and outlet of the channel. For example for the flow field in the top boundary (see Figure 1) the following conditions are used:

$$f_{4,n}= f_{2,n}, f_{7,n}= f_{7,5}, and f_{8,n}= f_6. \tag{18}$$

For the channel inlet (left main wall) Zou and He's boundary condition is used They introduced the below method for the calculation of unknown boundary conditions.

$$\begin{cases} \rho = \sum_{i=0}^{8} f_i \\ \rho u = \sum_{i} f_i e_i \end{cases} \tag{19}$$

On the assumption that the velocity on the inlet wall (u_w and v_w) is known, the rest of the numerical procedure is defined as below. In this special case, the inlet flow should be divided into parts and the below relations should be calculated for both of them separately.

$$\begin{aligned} \rho_w &= f_0 + f_1 + f_2 + f_3 + f_4 + f_5 + f_6 + f_7 + f_8 \\ \rho_w u_w &= f_1 + f_5 + f_8 - f_3 - f_6 - f_7 \\ \rho_w v_w &= f_2 + f_5 + f_6 - f_4 - f_7 - f_8 \end{aligned} \tag{20}$$

By implementation of the bounce-back rule in the inlet:

$$f_1 - f_1^{eq} = f_3 - f_3^{eq}, \tag{21}$$

$$f_1 = f_3 + \frac{2}{3}\rho_w u_w. \tag{22}$$

Finally, with the combination of the above relations, the unknowns at the channel inlet are calculated.

$$\rho_w = \frac{1}{1-u_w}\left[f_0 + f_2 + f_4 + 2\left(f_3 + f_6 + f_7\right)\right]$$

$$\begin{aligned} f_5 &= f_7 - \frac{1}{2}\left(f_4 - f_2\right) + \frac{1}{6}\rho_w u_w + \frac{1}{2}\rho_w v_w \\ f_8 &= f_6 - \frac{1}{2}\left(f_2 - f_4\right) + \frac{1}{6}\rho_w u_w + \frac{1}{2}\rho_w v_w \end{aligned} \tag{23}$$

For the channel outlet, the extrapolation boundary condition is used, where $n$is the lattice on the boundary.

$$f_i(n, j) = 2f_i(n-1, j) - f_i(n-2). \tag{24}$$

5. Results and discussion

In this study, the effect of a porous screen on nonuniform inlet velocity flow and heat transfer in a horizontal plane channel was considered using the LBM (Figure 1). The effects of the Darcy number and the variable porosity model were investigated on the flow field stabilization and convective heat transfer. The present computation focused on parameters with the following ranges: Da = 10^{-4} to 10^{-1}, $\varepsilon = 0.4$, Prandtl number = 0.7, and Reynolds number (Re) = 50.

To validate the numerical simulation, the flow and forced convection in a channel filled with or without (i.e. Poiseuille flow) a porous medium were simulated and compared with previous studies (Figures 3 and 4). Results showed good agreement in comparison with the previous studies of Narang and Hussain (1981) (Figure 3) and of Guo and Zhao (2002) and Alkam et al. (2002) (Figure 4).

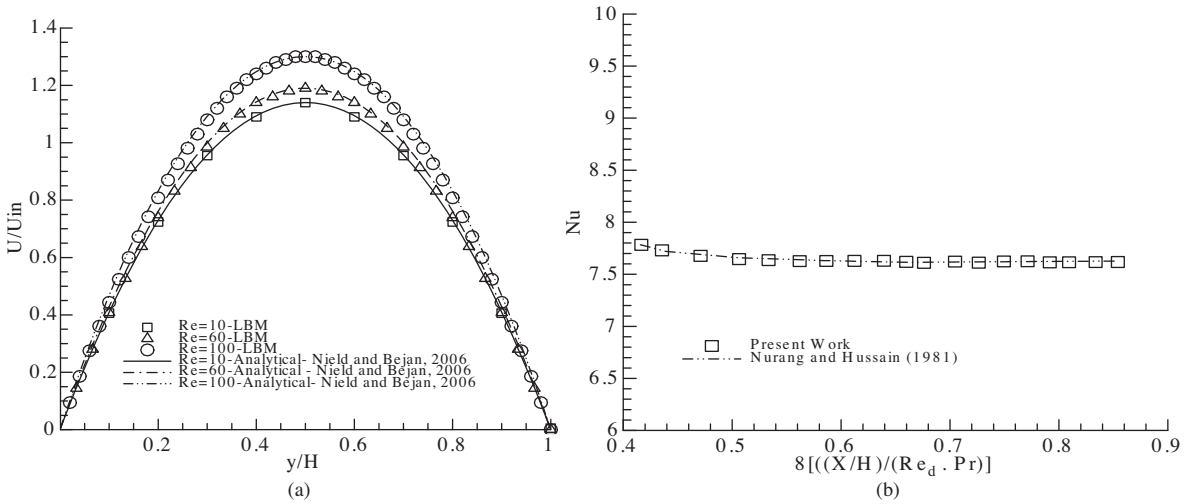

Figure 3. (a) Velocity profile and (b) local Nusselt number distribution in Poiseuille flow for present study and previous studies.

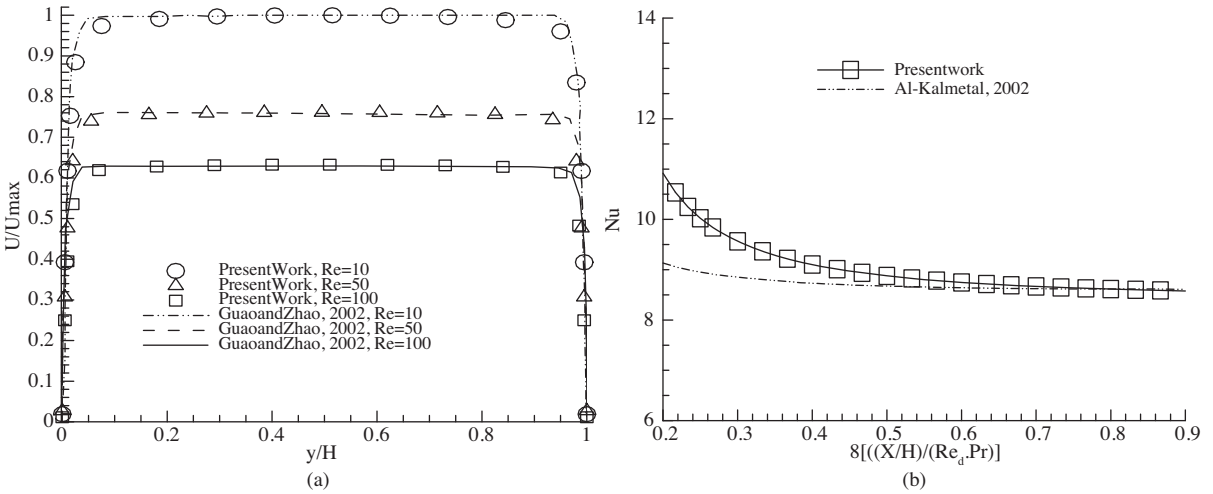

Figure 4. (a) Velocity profile and (b) local Nusselt number distribution in Poiseuille flow for present study and previous studies.

Some discrepancies exist between the present simulation and the results of Alkam et al. (2002) for local Nusselt number distribution (Figure 4). These are due to the difference between inlet velocity profiles, as a parabolic velocity profile was used by Alkam et al. and a uniform inlet velocity profile was used in this study.

To investigate the grid independency, the velocity profile was considered in the fully developed region of the channel filled by porous medium at 3 different grid points, (640 × 80), (800 × 100), and (960 × 120), at Re=50, Da = 10^{-2}, and $\varepsilon = 0.6$. It was observed that the grid point of (800 × 100) was sufficiently fine to ensure a grid-independent solution.

In a porous bed ?lling a channel or pipe with rigid and impermeable walls, there is a common increase in porosity as one comes near the walls. This is because the solid particles are not capable of standing or sitting together in a well-organized manner as elsewhere, because of the existence of the wall. Experiments show that porosity is a damped oscillatory function with respect to the distance from the wall, varying from a magnitude near unity at the wall to nearly core value at about 5 diameters from the wall (Nield and Bejan, 2006) (Figure 5). The notion of volume averaging over a REV breaks down near the wall, and most researchers have assumed a variation of the following form (Nield and Bejan, 2006):

$$\varepsilon = \varepsilon_\infty[1 + C.\exp(-N\frac{y}{d_p})], \tag{17}$$

where d_P is the particle diameter and C and N are experiential constants. Some experiments have indicated that appropriate values are $C = 1.4$ and $N = 5$ or 6 for a medium with $\varepsilon_\infty = 0.4$ (Cheng et al., 1991). Figure 6 shows the distributions of nondimensional velocity in the y direction for different values of x/H (x/H = 0.5, 0.7, 1) at Da = 10^{-3} and $\varepsilon = 0.6$. It was observed that the nonuniform inlet flow becomes stabilized after a porous layer and a homogeneous velocity distribution are obtained. For instance, before the porous screen (x/H = 0.5), the velocity gradient between y/H = 0.25 and y/H = 0.85 was about 65%, but this gradient reduced and reached nearly 40% after the porous screen (x/H = 0.7). The effect of the Darcy number on nondimensional velocity at a constant porosity is shown in Figure 7. The steadiness and uniformity of the velocity profiles are improved at lower values of the Darcy number. By paying attention to the definition of Da = K/H^2, it can be seen that the Darcy number decreases when the permeability is reduced. By paying attention to the permeability definition, it can also be seen that if the bubbles of porous media are very small or if they are poorly connected, the permeability will be low and the fluid will not flow through easily. Therefore, when the Darcy number and consequently the permeability decrease, the collisions among the fluid flow and the pores of the porous screen increase. Thus, the velocity profile becomes stable with decreases in the Darcy number. For constant Darcy numbers, the velocity profile is smoother for the variable porosity model in comparison with constant porosity. However, the velocity profile is most sensitive to any variation of porosity. The deviations between the variable and constant porosity models decrease with decreasing Darcy numbers. The instability of the velocity distribution is reduced and a homogeneous flow field is obtained with decreasing Darcy numbers (Figure 8). The local and average Nusselt numbers are calculated.

$$Nu = \frac{D_H}{\theta_w - \theta_m}\left.\frac{\partial\theta}{\partial y}\right|_{wall}, Nu_{avg} = \frac{1}{L}\int_0^L Nu\,dx, \tag{18}$$

Here, the nondimensional temperature (θ) is introduced as:

$$\theta = \frac{T - T_w}{T_{in1} - T_w}, \theta_m = \frac{T_m - T_w}{T_{in1} - T_w}. \tag{19}$$

In Eqs. (20) and (21), D_H is the hydraulic diameter and is specified as $D_H = 2H$, and θ_m is the dimensionless mean temperature. The bulk mean temperature (T_m) and mean velocity are calculated as follows:

$$T_m = \frac{1}{HU_m}\int_0^H uTdy, U_m = \frac{1}{H}\int_0^H udy. \tag{20}$$

The distribution of the temperature profile for variable and constant porosity is shown at different Darcy numbers in Figure 9. The temperature distribution is not expected to vary markedly, except near the wall.

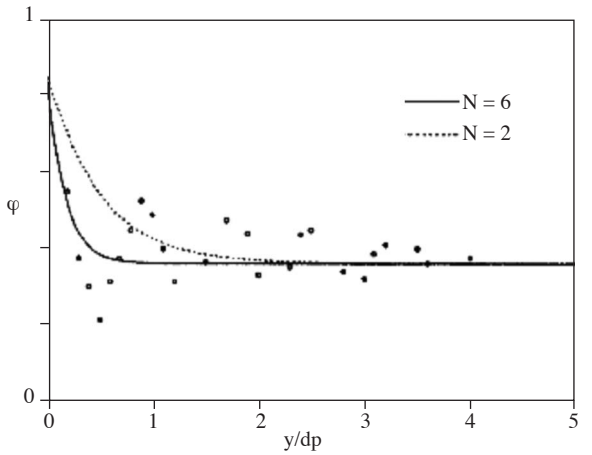

Figure 5. Variation of porosity near the wall (Nield and Bejan, 2006).

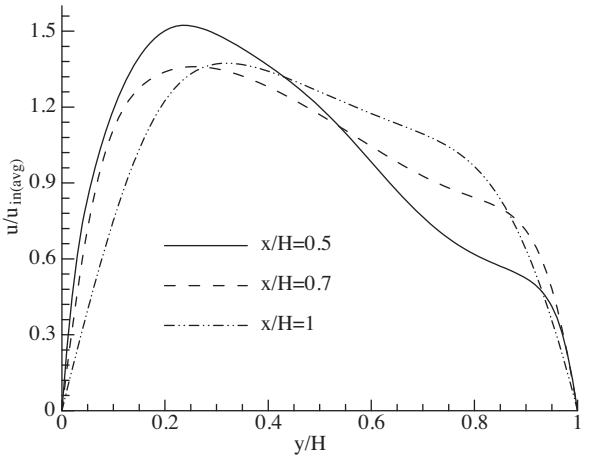

Figure 6. Axial velocity along the distance from the bottom wall at different locations for Da = 10^{-3}, ε = 0.6.

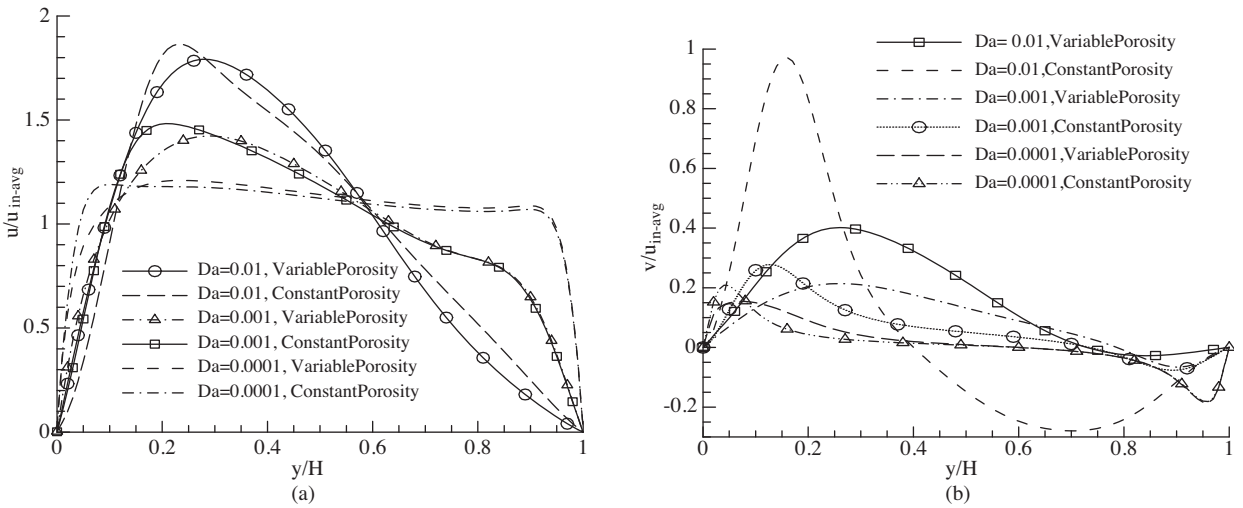

Figure 7. Distribution of axial (a) and vertical (b) velocity along the distance from the bottom wall for variable and constant porosity with respect to Darcy number variations at x/H = 0.7.

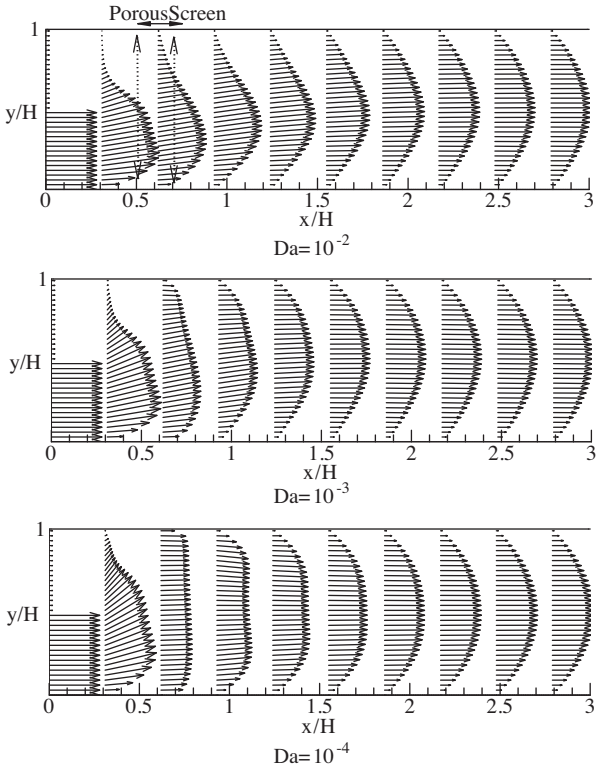

Figure 8. Velocity vector at different Da numbers at $\varepsilon = 0.4$.

The effect of the porous screen over the temperature distribution at different Da numbers is shown in Figure 10. It was observed that the maximum temperature gradient was decreased faster by the porous screen at lower Darcy numbers and, subsequently, better homogeneous temperature contours were created at smaller channel lengths.

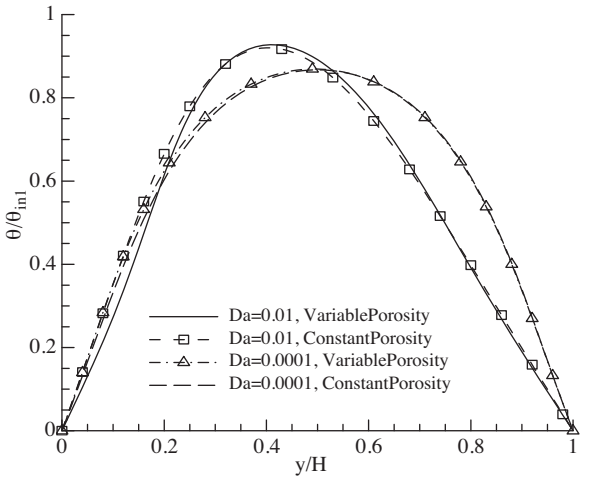

Figure 9. Distribution of temperature contours for variable and constant porosity at x/H = 0.7.

The effect of different Darcy numbers on the local Nusselt number is presented in Figure 11 for the bottom wall of the channel. The difference between the local Nusselt numbers is not very sensitive at different

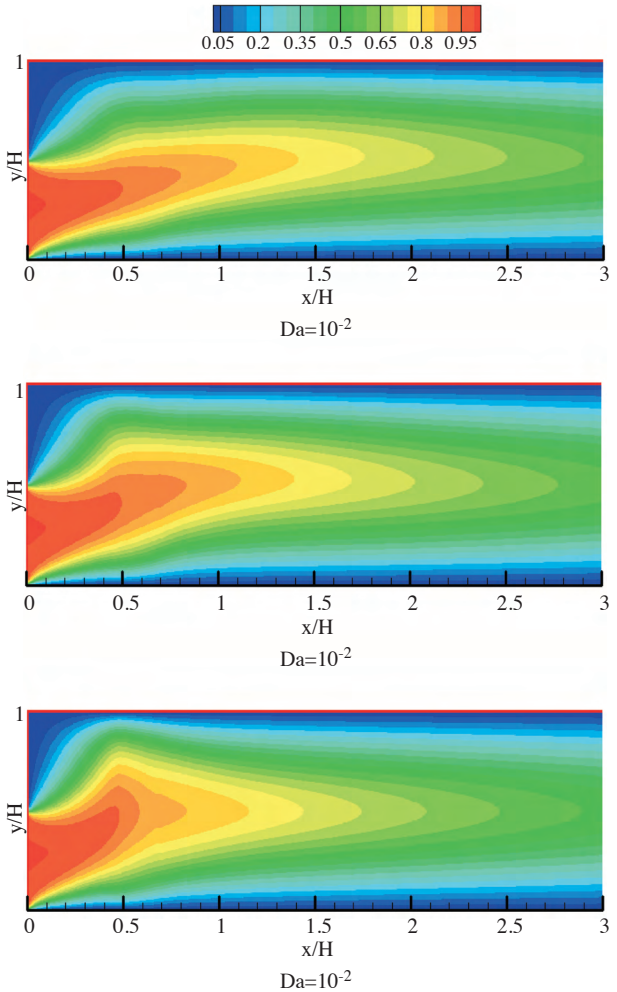

Figure 10. Distribution of the temperature contours at different Da numbers.

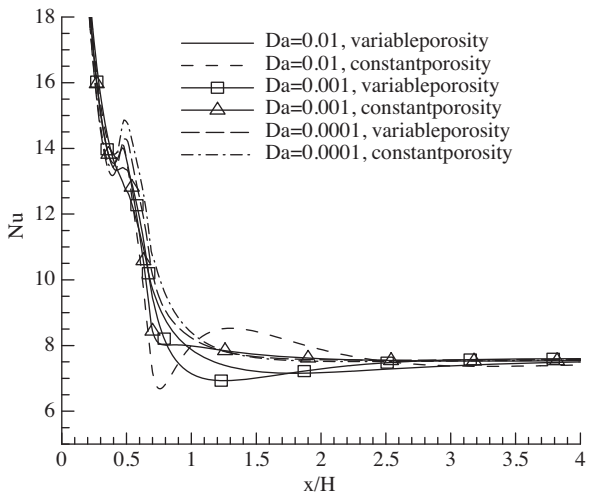

Figure 11. Local Nusselt number over the bottom wall for different Darcy numbers at $\varepsilon = 0.4$.

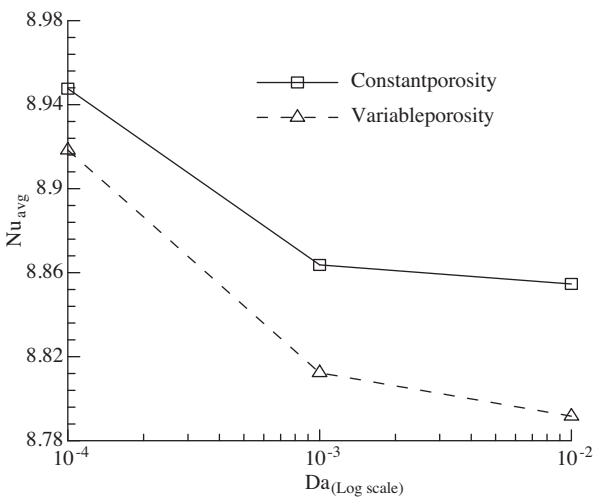

Figure 12. Average Nusselt number over the bottom wall for different Darcy numbers at $\varepsilon = 0.4$.

Darcy numbers. It can be observed that lower values of the Darcy number lead to higher values of the Nusselt number in the porous area. This is due to the rising of the temperature gradient near the wall. After the porous screen, the hottest fluid has the maximum Nusselt number. The average Nusselt number was plotted for different Darcy numbers at the bottom wall of the channel (Figure 12). The results of the variable and constant porosity models did not show observable differences in the local and average Nusselt numbers. However, it was observed that the results of these 2 models were close to each other, although using the variable porosity model led to a lower Nusselt number.

6. Conclusion

Flow in a horizontal plane channel partially filled with a porous screen with nonuniform inlet velocity and temperature was considered here. The LBM was employed for the solution of flow and heat transfer. A variable porosity scheme was used for modeling the actual manner of porosity on the porous region. Distributions of nondimensional velocity, nondimensional temperature, and local and average Nusselt number variations for the Darcy number and porosity were presented. The main observations were as follows:

-The flow behavior can be controlled using a porous screen.

-The nonuniformity of the flow and heat transfer is damped with decreasing Darcy numbers and porosity.

-The variable porosity model shows a stable velocity profile in shorter channel lengths in comparison with the constant porosity model.

-The deviations between constant and variable porosity models decrease at low Darcy numbers.

Nomenclature

x, y	Cartesian coordinates
Da	Darcy number, K/H^2
H	channel width
L	channel length
c	discrete lattice velocity
c_s	speed of sound in lattice
f_i^{eq}	equilibrium distribution function
c_s	speed of sound in lattice
Nu	local Nusselt number
Nu_{avg}	average Nusselt number
K_s	thermal conductivity of solid
K_f	thermal conductivity of fluid

Greek symbols

K	permeability of porous medium [m^2]
ε	porosity
υ	kinematic viscosity [Pa s^{-1}]
α	thermal diffusivity of porous medium [m^2 s^{-1}]
θ	dimensionless temperature (θ = T - T_{in}/T_{in} $-T_w$)
ω_i	weighting factor

Subscripts

avg	average
in	inlet
w	wall

References

Alazmi, B. and Vafai, K., "Analysis of Variable Porosity, Thermal Dispersion, and Local Thermal Nonequilibrium on Free Surface Flows Through Porous Media", Journal of Heat Transfer, 126, 389-399, 2004.

Alkam, M.K., Al-Nimr, M.A. and Hamdan, M.O.,"On Forced Convection in Channels Partially Filled with Porous Substrate", Heat and Mass Transfer, 38, 337-342, 2002.

Chandrasekhars, B.C. and Radha, N., "Effect of Variable Porosity on Laminar Forced Convection in a Uniformly Heated Vertical Porous Channel", Heat and Mass Transfer, 23, 371-377, 1988.

Cheng, P., Chowdhury, A. and Hsu, C.T., "Forced Convection in Packed Tubes and Channels with Variable Porosity and Thermal Dispersion Effects", in Convective Heat Mass Transfer in Porous Media (S. Kakaç et al., eds.), Kluwer, Dordrecht, 1991: pp. 625-653.

Chua, H.S., Yeh, C. and Chen, F., "Effects of Porosity Change of Gas Diffuser on Performance of Proton Exchange Membrane Fuel Cell", Journal of Power Sources, 123, 1-9, 2003.

Delavar, M.A., Farhadi, M. and Sedighi, K., "Effect of the Heater Location on Heat Transfer and Entropy Generation in the Cavity Using the Lattice Boltzmann Method", Heat Transfer Research, 40, 521-536, 2009.

Delavar, M.A., Farhadi, M. and Sedighi, K., "Numerical Simulation of Direct Methanol Fuel Cells Using Lattice Boltzmann Method", International Journal of Hydrogen Energy, 35, 9306-9317, 2010.

Ergun, S., "Fluid Flow through Packed Columns", Chemical Engineering Progress, 48, 89-94, 1952.

Guo, Z., Kim, S.Y. and Sung, H.J., "Pulsating Flow and Heat Transfer in a Pipe Partially Filled with a Porous Medium", International Journal of Heat and Mass Transfer, 40, 4209-4218, 1997.

Guo, Z. and Zhao, T.S., "Lattice Boltzmann Model for Incompressible Flows through Porous Media", Physical Review E, 66, 036304, 2002.

Guo, Z., Zheng, C. and Shi, B., "Discrete Lattice Effects on the Forcing Term in the Lattice Boltzmann Method", Physics Rev. E, 65, 046308, 2002a.

Guo, Z., Zheng, C. and Shi, B., "An Extrapolation Method for Boundary Conditions in Lattice Boltzmann Method", Physics of Fluids, 14, 2007-2010, 2002b.

Hamdan, M.O., Al-Nimr, M.A. and Alkam, M.K., "Enhancing Forced Convection by Inserting Porous Substrate in the Core of a Parallel-Plate Channel", International Journal of Numerical Methods for Heat and Fluid Flow, 10, 502-517, 2000.

Jen, T.C. and Yan, T.Z., "Developing Fluid Flow and Heat Transfer in a Channel Partially Filled with Porous Medium", International Journal of Heat and Mass Transfer, 48, 3995-4009, 2005.

Jiang, P.X., Li, M., Ma, Y.C. and Ren, Z.P., "Boundary Conditions and Wall Effect for Forced Convection Heat Transfer in Sintered Porous Plate Channels", International Journal of Heat and Mass Transfer, 47, 2073-2083, 2004.

Kaviany, M., "Laminar Flow through a Porous Channel Bounded by Isothermal Parallel Plates", International Journal of Heat and Mass Transfer, 28, 851-858, 1985.

Kim, S.J. and Vafai, K., "Analysis of Natural Convection about a Vertical Plate Embedded in a Porous Medium", International Journal of Heat and Mass Transfer, 32, 665-677, 1989.

Liou, M.F., A Numerical Study of Transport Phenomena in Porous Media, PhD Thesis, Case Western Reserve University, 2005.

Mohammad, A.A., Applied Lattice Boltzmann Method for Transport Phenomena, Momentum, Heat and Mass Transfer, Sure Printing, Calgary, 2007.

Nield, D.A. and Bejan, A., Convection in Porous Media, 3rd edition, Springer, New York, 2006.

Narang, B.S. and Hussain, N.A., "Analysis of Laminar Forced Convective Heat Transfer in the Entrance Region of a Flat Duct with Uniform Wall Temperature", American Society of Mechanical Engineers and American Institute of Chemical Engineers, 20th National Heat Transfer Conference, 1981.

Özdemir, M. and Özgüç, A.F., "Porosity Variation and Determination of REV in Porous Medium of Screen Meshes", International Communications in Heat and Mass Transfer, 24, 955-964, 1997.

Poulikakos, D. and Kazmierczak, M., "Forced Convection in a Duct Partially Filled with a Porous Material", Journal of Heat Transfer, 109, 653-662, 1987.

Satyamurty, V.V. and Bhargavi, D., "Forced Convection in Thermally Developing Region of a Channel Partially Filled with a Porous Material and Optimal Porous Fraction", International Journal of Thermal Sciences, 49, 319-332, 2010.

Seta, T. and Kono, K., "Thermal Lattice Boltzmann Method for Liquid-Gas Two-Phase Flows in Two Dimension", JSME International Journal Series B, 47, 572-583, 2004.

Seta, T., Takegoshi, E., Kitano, K. and Okui, K., "Thermal Lattice Boltzmann Model for Incompressible Flows through Porous Media", Journal of Thermal Science and Technology, 1, 90-101, 2006.

Spaid, M.A.A. and Phelan, F.R., "Lattice Boltzmann Methods for Modeling Microscale Flow in Fibrous Porous Media", Physics of Fluids, 9, 2468-2474, 1997.

Succi, S., Foti, E. and Higuera, F., "3-Dimensional Flows in Complex Geometries with the Lattice Boltzmann Method", Europhysics Letters, 10, 433-438, 1989.

Zou, Q. and He, X., "On Pressure and Velocity Boundary Conditions for the Lattice Boltzmann BGK Model", Physics of Fluids, 9, 1591-1598, 1997.